UCRL-7766

University of California

Ernest O. Lawrence
Radiation Laboratory

AN IMPULSE ACCELEROMETER

Livermore, California

DISCLAIMER

UCRL-7766
Instruments, UC-37,
TID-4500 (30th Ed.)

UNIVERSITY OF CALIFORNIA
Lawrence Radiation Laboratory
Livermore, California

Contract No. W-7405-eng-48

AN IMPULSE ACCELEROMETER

William E. Nelson, Jr.
G. Wayne Brown

March 12, 1964

Printed in USA. Price 75 cents. Available from the
Office of Technical Services
U. S. Department of Commerce
Washington 25, D.C.

CONTENTS

AN IMPULSE ACCELEROMETER

William E. Nelson, Jr., and G. Wayne Brown

Lawrence Radiation Laboratory, University of California
Livermore, California

March 12, 1964

ABSTRACT

Contemporary accelerometers fall into two general categories, mechanical deformation and electronic transducer. The first type can be small and rugged but it has the disadvantage of reading out only an acceleration level — which must be regarded as a "figure of merit" depending on the relationship between the dynamic response of the accelerometer and the nature of the input excitation. The electronic transducers are capable of accurate acceleration input monitoring, if properly used, but require conditioning and readout equipment for which there often is no space or power.

This report describes an accelerometer which offers some of the advantages of each of the above categories. It is relatively small and rugged and requires no conditioning or readout equipment during operation. Readout consists of an "equivalent" square wave with an acceleration level and pulse interval time. The instrument can be utilized to measure square wave accelerations directly, or, if a wave shape is known, its output data can be mathematically transformed to the type of "g-signature" actually measured.

The particular geometry discussed was shown to be useful for acceleration ranges of 100-250 g's and 150-450 g's. These ranges can be extended by modification of certain design parameters which are discussed herein.

INTRODUCTION

A great deal of effort has been expended in recent years toward improving techniques of design for shock and impact loading. Any design technique must rely on a knowledge of the forces which will be applied to the prospective system, and this knowledge can only be obtained by making suitable measurements under the actual loading conditions. Forces which arise under shock and impact loading conditions are primarily due to accelerations (both positive and negative) on a system, so it becomes an obvious necessity to be able to measure these accelerations.

There are several means available for measuring accelerations. For example, electronic accelerometers have been developed to a high degree. However, their use requires a power supply and some type of pickup system, thus presenting disadvantages for applications where weight and space are at a premium. (See Ref. 4)

Various types of "peak-reading" accelerometers have also been developed, usually operating on some sort of mechanical deformation principle (see refs. 1-3). These instruments, however, are only capable of indicating the magnitude of the highest acceleration to which they are subjected, and can yield no information about the time of its application. They offer the advantages of compactness, ruggedness, simplicity, and no requirement for external instrumentation, all of which are highly desirable for limited space applications.

It is evident that there is a need for an acceleration measuring device with the advantages of the peak-reading accelerometers but which will make measurements more on the order of the electronic instruments, which can usually give a complete acceleration-time history. Such an accelerometer would be capable of indicating acceleration magnitudes and also of recording some information about the time pulses during which the accelerations are applied.

DESIGN OBJECT

The object of this project was to design an "impulse" accelerometer, an instrument which will indicate magnitudes of acceleration and time duration of acceleration pulses.

Additional desirable requirements for this design are that it should be rugged, compact, reliable, and should require no external instrumentation to

obtain the required data. While all of these requirements are essential to a successful final design, some of them are secondary to the basic problem of producing a system that will measure the desired parameters. Therefore the emphasis in this project has been placed on achieving a working system; the objectives of maximizing reliability and minimizing size have been left for future efforts.

METHOD OF SOLUTION

The method that has been used to satisfy the project objective was first proposed by G. Wayne Brown, Associate Professor of Mechanical Engineering at the University of California, Berkeley. This method consists in utilizing the properties of a nonlinear spring mass system in response to an acceleration pulse. The basic technique is to compare the effect of the same acceleration on two different masses in the manner in which they permanently deform coupons of aluminum foil cellular material – popularly known as "honeycomb." The honeycomb reacts as a nonlinear spring in that it exhibits a nearly constant force-deflection relationship after it has been initially failed, or "precrushed."

A theoretical analysis of this system (see Appendix I) shows that it is possible to measure the deformations of two similar coupons by two different masses and then, taking a deformation ratio and a deformation difference, go to two preplotted curves and obtain the magnitude of the acceleration to which the system had been subjected and the duration of time over which it was applied. The two curves in question are plotted by substituting the proper constant parameters of each system into the relationship obtained by solving the differential equation of motion for the system. The form of the curves turns out to be a hyperbola for the acceleration plot and a straight line for the curve combining acceleration and time.

It must be pointed out here that one of the basic assumptions made in the theoretical analysis was that the input acceleration was a constant for a finite period of time, or a square wave. This assumption has the effect of causing the data obtained from the system to define an "equivalent" square wave. This equivalent wave will have the same area as the actual input acceleration pulse and will be applied over the same length of time. In other words, this system will yield an average acceleration over the time interval of the pulse.

It is herein proposed that, in lieu of a complete acceleration-time trace, the equivalent square wave is the most significant indication of the cumulative forces which have been applied to the system. If the nature of the input wave is known, of course, the area and time duration of the pulse are sufficient information to allow a calculated acceleration-time history to be found. Also, if the peak acceleration could be obtained from some other source, it might be possible to combine that information with the pulse area and duration and extrapolate the true shape of the pulse. In any case, the equivalent square wave provides the only means by which a single value of acceleration and a single value of time can be significant in describing the reaction of a system to any type of input.

ACCELEROMETER DESIGN

Several factors were active in influencing the final design of the accelerometer. First of all, let us consider the equation for the deformation ratio which is derived in Appendix I:

$$\frac{y_1}{y_2} = \left(\frac{am_1}{\sigma_1 A_1} - 1\right) \Big/ \left(\frac{am_a}{\sigma_2 A_2} - 1\right) .$$

It can be seen that the numerator of this equation provides a definition of the least acceleration under which the first mass will deform the honeycomb coupon. This occurs when $am_1/\sigma_1 A_1 = 1$, or, if the acceleration is expressed in g's, $a_{min} = \sigma_1 A_1 / w_1$. If we assume that the first mass is the lighter of the two, then this term will set the minimum acceleration for which the system will respond. A maximum sensitivity will be obtained when the honeycomb crushing strength, σ_1, and the deformation area, A_1, are minimized and the weight of the first mass, w_1, is maximized. Since other considerations govern setting the size of the first mass, the deformation area was the most effective parameter for adjusting the sensitivity. The honeycomb crushing strength, for this project at least, was selected more on a basis of availability than desirability.

An arbitrary thickness of 1 inch was arrived at for the honeycomb, through consideration of the effect of this dimension on the overall size of the system. Since a suitably large piece of scrap honeycomb was obtained with this thickness and with the minimum available cell size of 1/8 inch, its

crushing strength was selected as a basis for the design. The crushing strength of this particular material after initial failure turned out to be approximately 300 psi.

Minimization of the deformation area proved to be a direct function of the honeycomb cell size. Since the minimum cell size manufactured for this material is 1/8 inch, it was this size that was selected so as to provide the maximum number of cell walls per unit area of deformation. The area of deformation was then fixed as a circular area with 1/2 inch diameter. It was felt that this would be the minimum practical area that would crush enough cells to be relatively free of scatter effects in the resulting data due to cell nonuniformity. Setting this dimension allowed the shape of the honeycomb coupons to be fixed – as cubes with all three sides 1 inch in length. This shape was large enough in top surface area to allow a 1/2-in.-diam plunger to penetrate the coupon without any varying edge effects. It was decided to use a plunger so as to assure a constant area of deformation, since the honeycomb is difficult to cut to accurate dimensions across the cells.

Once the size of the coupons had been fixed, it was possible to design the rest of the system around their dimensions. The outer accelerometer cases were fabricated in the form of hollow cylinders, with an upper chamber in which the masses could move up and down and a lower chamber in which the coupons could be suitably restrained and positioned. A 1/2-in.-diam passage between the two chambers was cut to allow the plunger, which was to be a part of the mass itself, to penetrate the coupon in the space below. Ends of the hollow cylinders were closed by means of threaded end plates, one of which contained a mounting stud for the whole assembly. This arrangement allowed the coupons to be easily changed during the verification of the system without the necessity of disassembling the rest of the unit. Figure 1 is an exploded view of the entire assembly, while Fig. 2 shows the coupon chamber with the plunger partially extended. Figures 3-6 show the manner in which the coupons were penetrated by the plungers, including the effects of two different masses under the same acceleration.

The masses themselves were designed with several objects in mind. First of all, the largest mass was designed to give the maximum weight for the space available, considering that cold-rolled steel was the only readily obtained material. Two other masses were then fabricated so as to achieve ratios between their weights of approximately 1.3 and 2.0. This was done so that verification could be obtained for two different sets of theoretical curves.

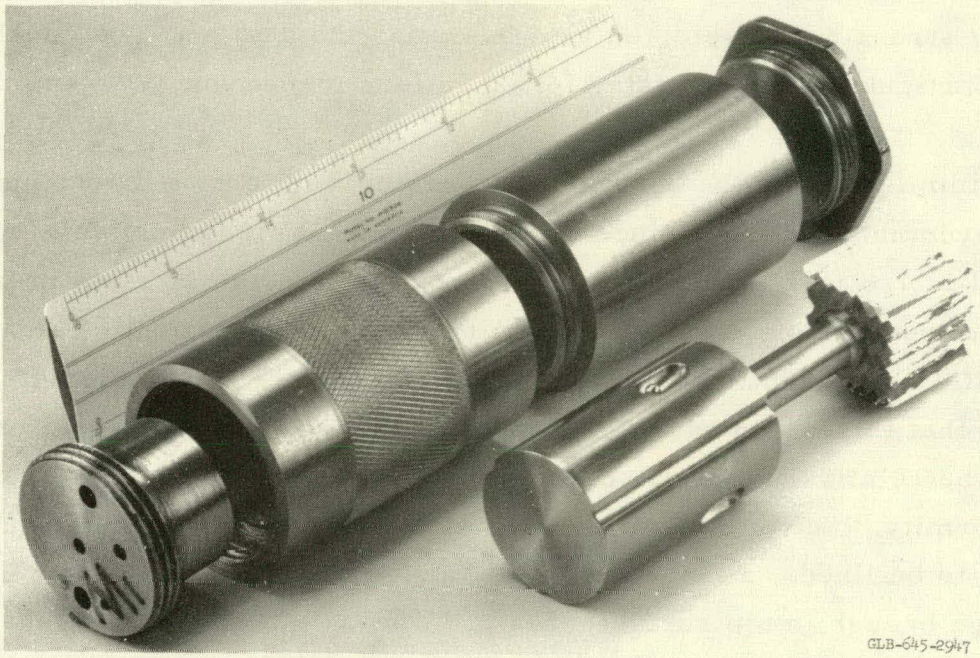

Fig. 1. Exploded view of accelerometer assembly. Items are, from left to right: Upper end plate with spacer attached, two-piece outer accelerometer case, bottom end plate with mounting stud (not in view), and in the foreground, the mass (with ball-check and venting groove), and an aluminum honeycomb coupon.

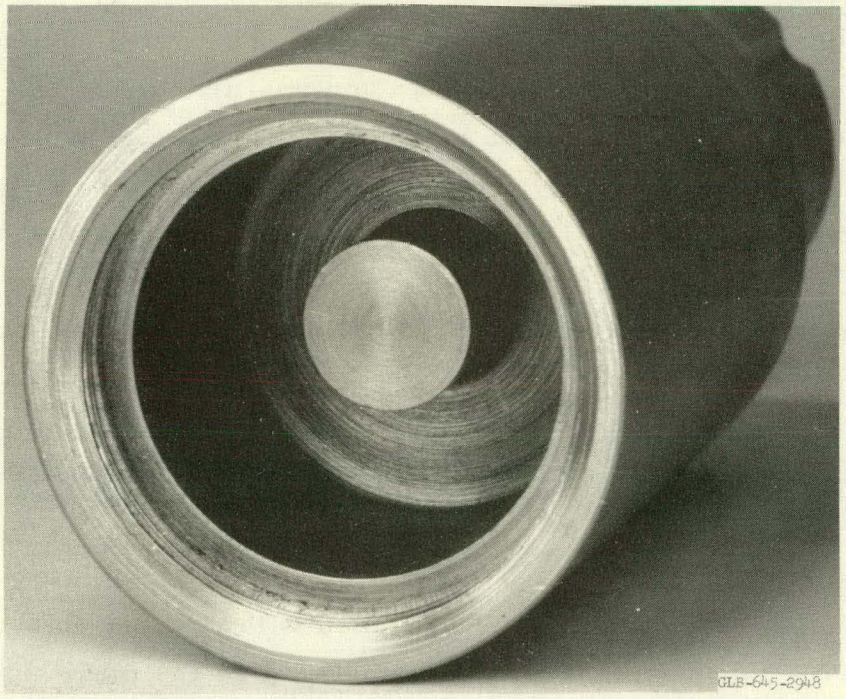

Fig. 2. End view showing chamber for aluminum honeycomb coupons. Note the plunger foot which is in an approximately half-extended position. In the initial position, this plunger extends 1/16 in. into the chamber, so as to precrush the coupon when the bottom plate is screwed in.

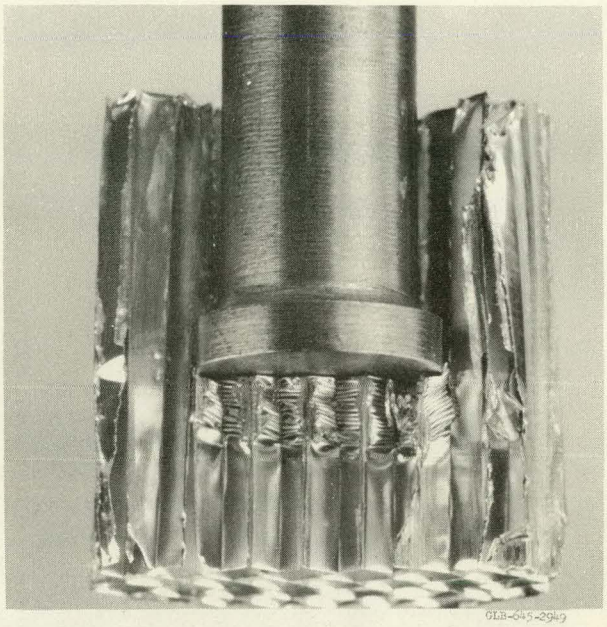

Fig. 3. Cutaway view of the plunger penetrating a honeycomb coupon. Note the characteristic wavelike mode of failure as buckling progresses beneath the foot of the plunger. The lip on the bottom of the plunger is to reduce the possibility of side-wall friction retarding its travel.

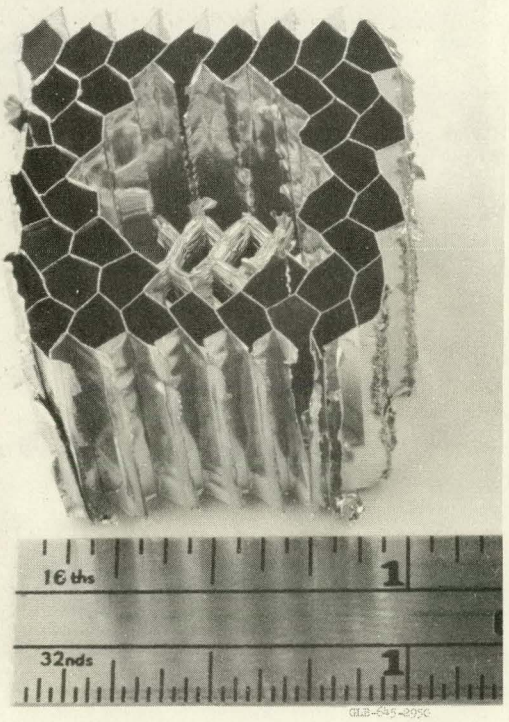

Fig. 4. Top view of an aluminum honeycomb coupon which has been deformed in a drop test. Note the variety of initial cell shapes, and how the cells maintain their shapes as the buckling progresses down through the coupon.

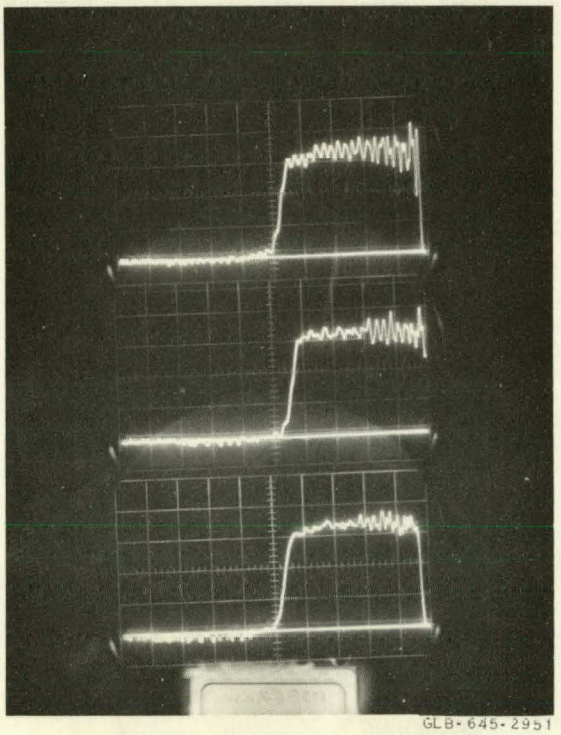

Fig. 5. Typical square-wave acceleration traces for three different drops. Note that the initial rise (on the right side of the photographs) is slightly steeper than the dropoff. The oscillations along the top of the traces are at a frequency of approximately 4000 cps, and are apparantly due to reverbations in the case of the control accelerometer.

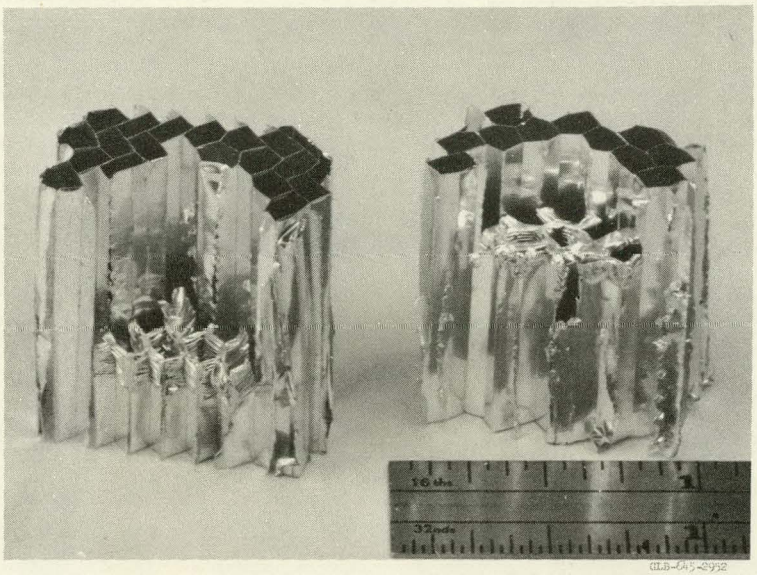

Fig. 6. Cutaway views of two coupons which were deformed under the same acceleration pulse. The deformations shown here were for an acceleration pulse of approximately 400 g's over a time period of approximately 1.2 msec.

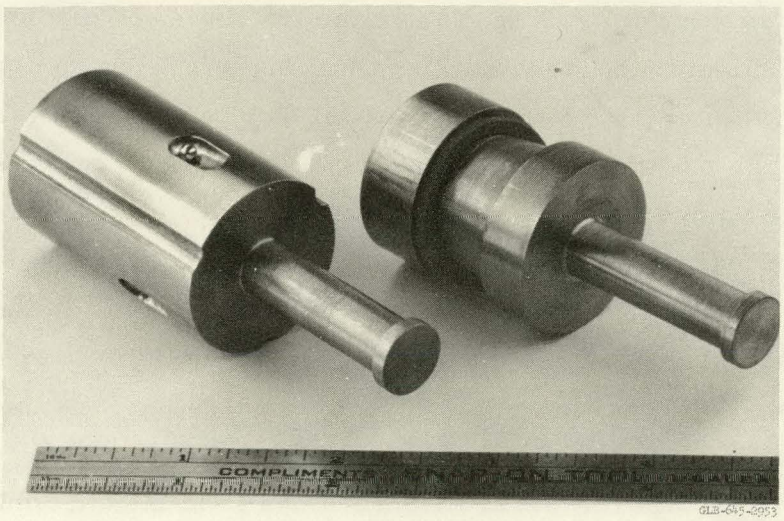

Fig. 7. Comparison view of the final (on the left) and initial design of the masses. Note the location of the ball-check seats and the ventilating groove on the newer design. The initial design required experimental ball-check seat angle cutting, which removed unnecessary material.

Positive rebound prevention was incorporated in the design by means of a ball-check mechanism, which operated between the mass and the accelerometer case. This mechanism, which consisted of small steel balls resting on tapered seats cut into the masses themselves, allowed the masses to move downward freely, but immediately locked if the mass attempted to bounce back upward. The masses were reset in their starting positions by turning the whole unit upside down and rotating the plunger until the ball-check unlocked and the mass dropped back to its starting position. Longitudinal grooves were also cut into the masses to allow airflow past them as they moved downward in their chambers. Figure 7 shows the initial and final shapes which were evolved for the masses.

It was mentioned above that the honeycomb must be initially failed, or "precrushed," before it will demonstrate the desired constant force-deflection characteristic. This is due to the fact that the honeycomb has a compressive strength that may be 40 to 60% higher than the nearly constant crushing strength that it demonstrates after it has initially failed. A means was found by which the actual precrushing was accomplished by the accelerometers themselves. This was done by attaching spacers to the end plates above the masses so that when the masses rested against these spacers the ends of their plungers projected into the coupon chambers approximately 1/16 in. When the coupons were placed in their spaces and the bottom end plates screwed in until they bottomed out, the projecting plungers were forced into the coupons – thereby accomplishing the precrushing. These built-in deflections, which had been found be experiment to be sufficient, were then a constant for each accelerometer. Once they were initially ascertained, it was no longer necessary to make preliminary measurements of the coupons, a factor which resulted in considerable savings in time. The location of the spacers on the upper end plates can be seen in Fig. 1.

This summary of the design, while not in actual chronological order of accomplishment, does reflect the criteria that led to the finished system. This system is theoretically capable of measuring accelerations from 100 to 1000 g's and time pulses up to 10 msec in duration; however, limitations in the testing facility placed a maximum figure of 600 g's on the experimental verification.

TESTING FACILITY

The basic method used to verify the theoretical analysis of the accelerometer system was to subject it to a known acceleration over a known length of time and compare the resulting deformation difference and deformation ratio with those predicted by the theory. The facilities used to accomplish this verification are located in the Dynamics Laboratory in the Mechanics Building at the University of California, Berkeley, California.

Accelerations (or, more accurately, decelerations) were achieved by means of a 22-foot drop tower. This drop tower consists basically of an aluminum drophead, a supporting carriage with an electrically actuated release mechanism, two vertical guiding cables, and a steel anvil upon which various materials can be placed to decelerate the drophead.

The drophead contains provisions for attaching the experimental accelerometers, an electronic control accelerometer, and various types of anvil strikers. The initial position of the system for each drop is established by raising the carriage, with drophead attached, to the desired height by means of a nylon cord and pulley arrangement. The carriage can be raised to and fastened at any desired position, the height of which is indicated by marks on one of the guide cables at 1-foot intervals. The drophead is then released by means of a push-button-actuated solenoid which opens a trigger mechanism. Figure 8 shows the arrangement and physical details of the drophead and carriage assembly, with the experimental accelerometers attached.

Control data was collected by means of a Statham resistance-wire-type accelerometer, rated at ±1000 g's, which was fastened to the drophead. This instrument was connected to an Ellis dc bridge power supply, which in turn was attached electrically to a Tektronix oscilloscope. The oscilloscope traces were recorded by means of a Polaroid camera mounted directly on the instrument. These traces were triggered by means of a battery-powered circuit which contained a pencil lead connected in a parallel resistance loop. This pencil lead was mounted on a special bracket on the drop tower anvil, so that a striker on the descending drophead would break the lead and cause a pulse to trigger the oscilloscope trace. The circuit for obtaining the control data is shown in Fig. 9, and the entire experimental facility is shown in Fig. 10.

Accuracy in performing measurements on the coupons was assured by the use of a Pratt & Whitney Supermicrometer to obtain all such data.

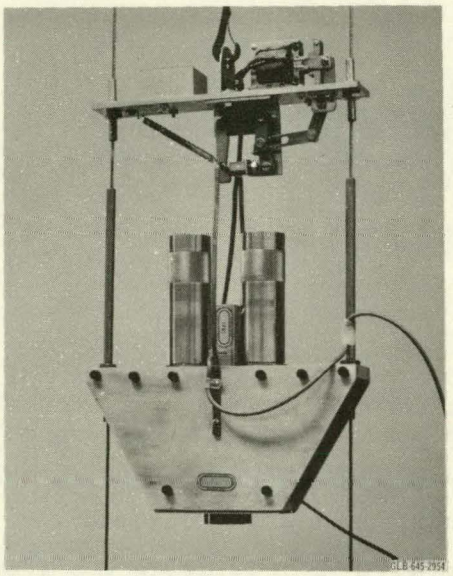

Fig. 8(a). Close-up view of the drophead and carriage assembly. Included are (from top to bottom): The support carriage with its solenoid-operated release mechanism; the drophead with the two experimental accelerometers in place on each side of the Statham accelerometer, and with the small striker protruding from the bottom.

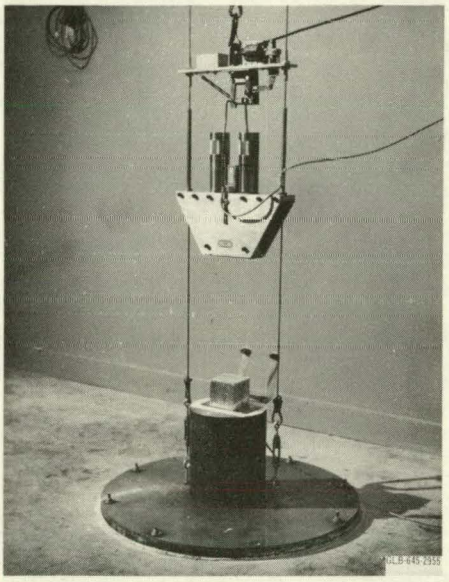

Fig. 8(b). Composite view of the entire drop tower. Note the honeycomb block on the anvil below the carriage and drophead assembly. Directly behind the honeycomb block is the pencil lead, in its supporting bracket, which triggers the oscilloscope trace when it is broken by the descending drophead. The guide cables are attached by means of turnbuckles to the large steel plate at the base, which is set in hydrostone. The bracket on the wall in the background is for securing the nylon cable which supports the carriage and drophead. In this view, as in most of the actual drops, the bottom of the drophead itself is being used as a striker.

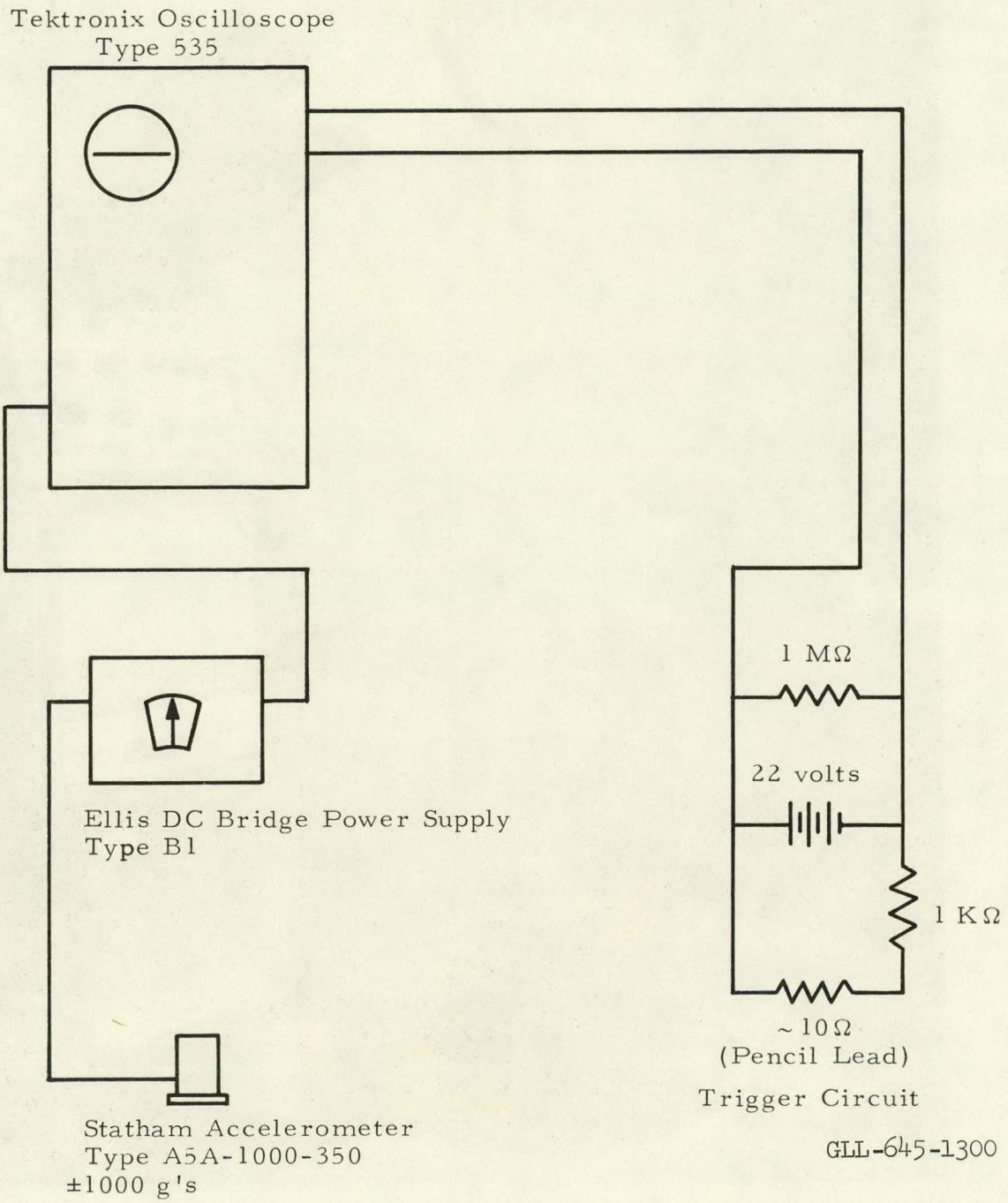

Fig. 9. Control data circuit diagram.

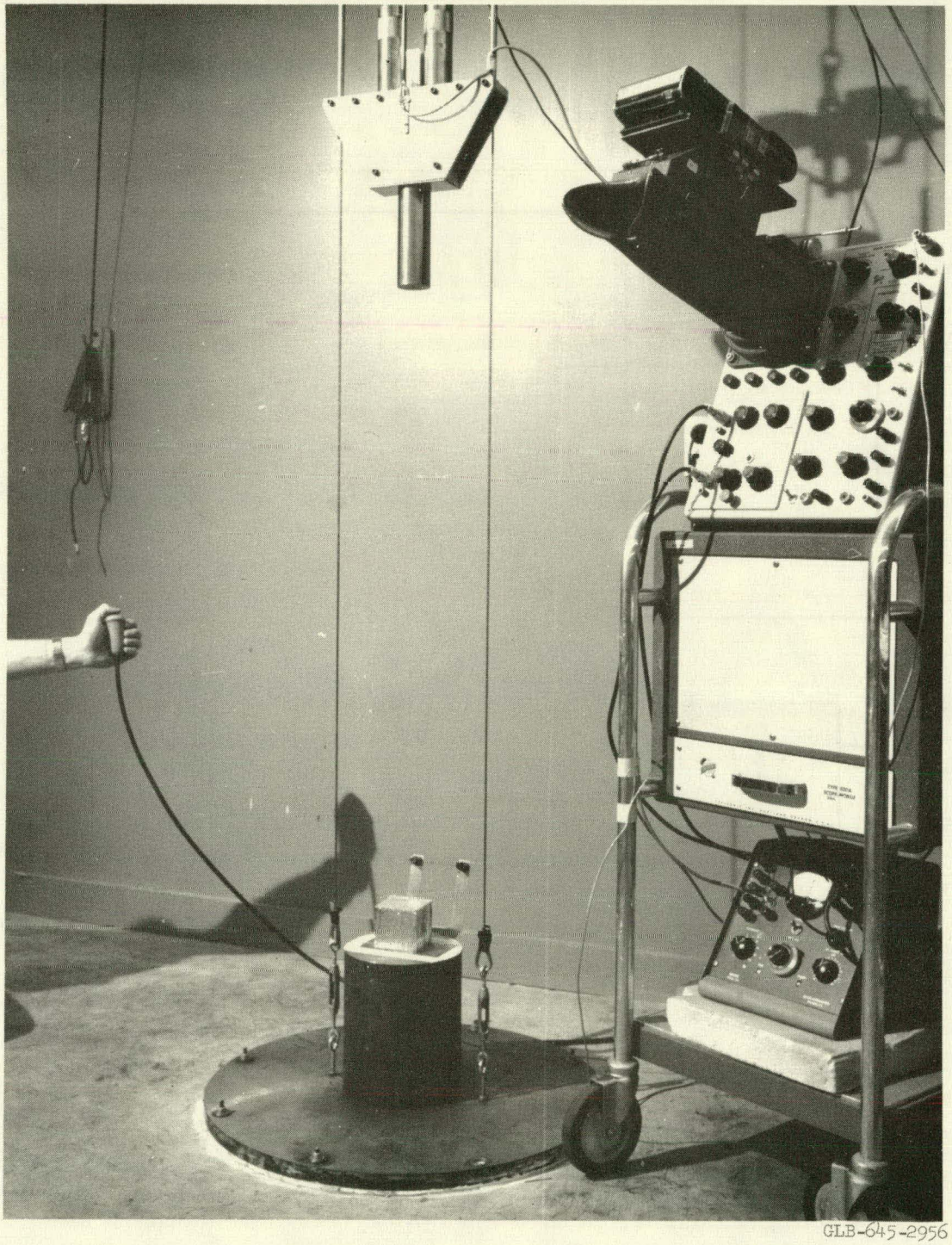

Fig. 10. Composite view of the experimental facility, showing (from left to right) the drophead release button, the drop tower, and the instrumentation cart. The cart accommodated the oscilloscope, with attached Polaroid camera, the triggering circuit package with its battery, and the dc bridge power supply. Note the 6-inch plunger on the drophead, which was used for some of the drops at low g-loadings and long time pulses.

EXPERIMENTAL PROCEDURE

The actual process of verifying the theoretical analysis was started by plotting approximate theoretical curves for the known parameters of the system. Data points were then accumulated by making 78 drops on the tower at varying g-loads and lengths of time. These drops were approximately evenly divided between the two available mass ratios, 1.3 and 2.0. A control plot was maintained so that the data points would reasonably cover the range available for the tests.

Since the theoretical analysis was based on the assumption of a square-wave acceleration input, the drops were made under conditions as close to this as could be achieved. This was successfully accomplished by using blocks of precrushed honeycomb to decelerate the drophead, thereby utilizing the aforementioned constant force-deflection characteristic to generate a constant acceleration-time characteristic. The accelerations could then be varied at will be merely changing the area of deformation. The times could be varied at any given acceleration by merely changing the drop height.

Several arrangements were attempted for varying the available striker area of the drophead, but only one was generally successful. In order to eliminate resonant reverberations in the drophead it was found that the bottom of the drophead itself was the best striker. This area was limited, however, and it and the strongest honeycomb available could only subject the system to a deceleration of 600 g's. For this reason, as mentioned before, the experimental verification was conducted over a range from 100 g's (the minimum to which the system could respond) to 600 g's – a range that is considered to be quite adequate for the purposes of this investigation.

The chronological sequence of events during a set of drops was as follows: Desired g-levels were picked (usually varying in increments of 25, 50, or 100 g's) and honeycomb blocks were cut to the proper size to achieve these levels. The honeycomb blocks were then precrushed, for the same reason as the coupons, in a compression testing machine. Coupons which had been previously cut to proper size were then placed in the accelerometers, which were then screwed tightly shut so as to precrush the coupons. The accelerometers were then placed in position on the drophead, and the whole assembly was raised to the desired drop height. A pencil lead was next placed in the trigger support bracket, and the proper honeycomb block was placed on the anvil. The trigger was then "set" in the oscilloscope, the

camera shutter was opened, and the solenoid release button was pushed to make the drop. The coupons were then removed from the accelerometers for later measuring, and the whole process was repeated for the next drop.

Drops were made in sets of three for each g-level and time pulse length, so as to minimize the effects of statistical variations in the honeycomb. Data was used only from those drops for which there was a picture of the acceleration trace. The coupons were kept in egg cartons, in numbered spaces, after they were removed from the accelerometers, and the coupon numbers were noted on the backs of the corresponding acceleration trace photographs. This procedure assured that the proper control data was compared with the proper coupon deformations. These deformations, as has been mentioned before, were measured by means of a Supermicrometer so as to minimize any possible effects due to measuring inaccuracy.

DISCUSSION OF RESULTS

The result of the experimental investigation are presented graphically in Figs. 11 and 12 for the two mass ratios, 1.3 and 2.0. Theoretical curves, which are explained below, are also plotted on the same graphs.

It is apparent from these plots that the general distribution of the experimental points does fall into the predicted patterns. Both the acceleration curves fall into a general hyperbolic shape, and both time diagrams show an approximate straight-line distribution. It is also evident, however, that there is a definite scatter in the data points throughout the ranges of the investigation. It is of interest to note that the best verification of an acceleration curve was for the mass ratio 1.3, while the best agreement of a time diagram with the theory was for the 2.0 ratio. These two examples are not enough evidence to be used as foundations for any predictions along this line, however.

A comment should be made at this point about how the theoretical curves were obtained. It was mentioned previously that approximate theoretical curves were plotted and used for data control purposes during the course of the experimental investigation. After a substantial amount of data had been obtained it became evident that there was a definite scatter in the results, but also that the data was consistently distributed above the acceleration curves and below the time curves. The experimental methods and equipment were carefully examined at this point to try and find a cause for this behavior. The

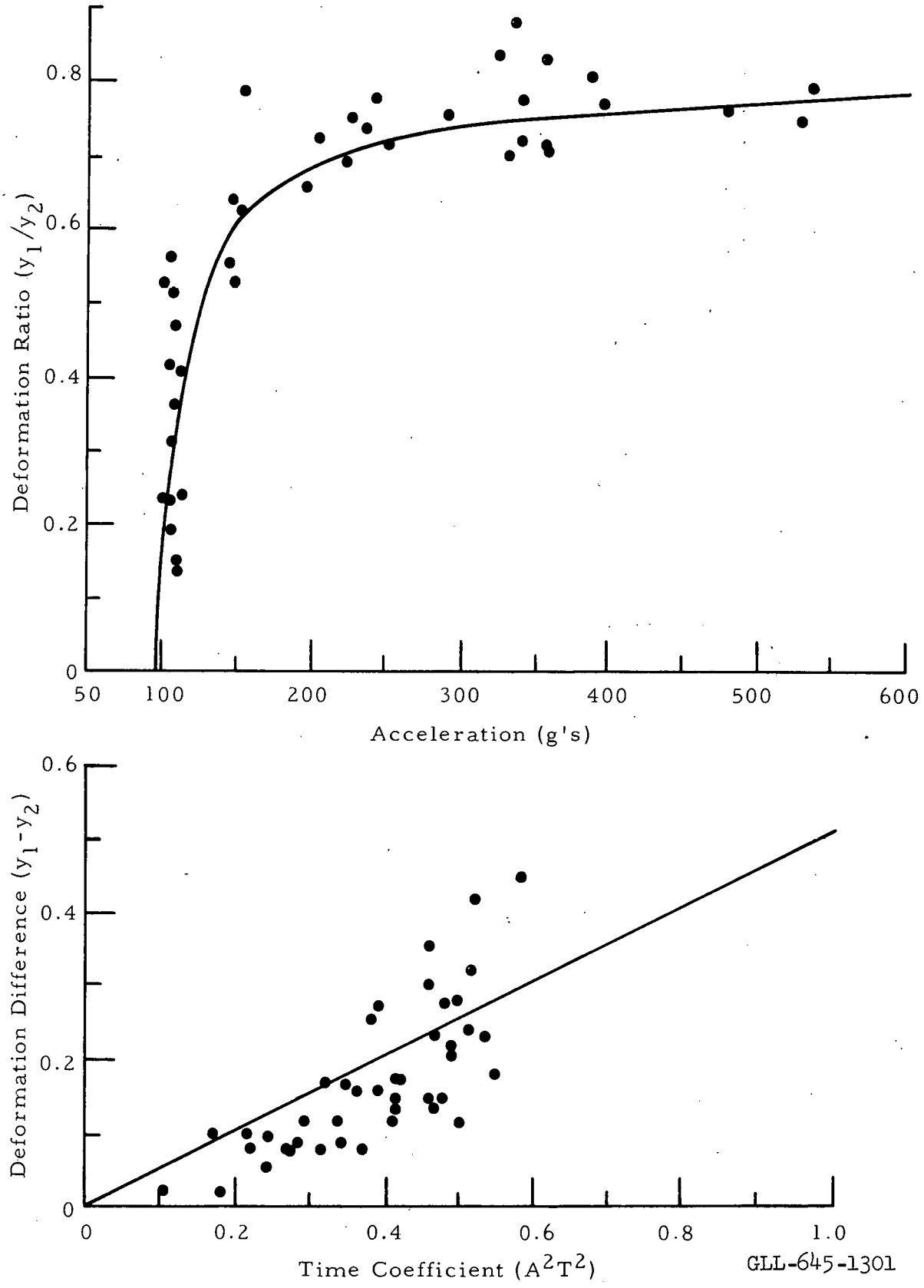

Fig. 11. Accelerometer data charts, mass ratio 1.3.

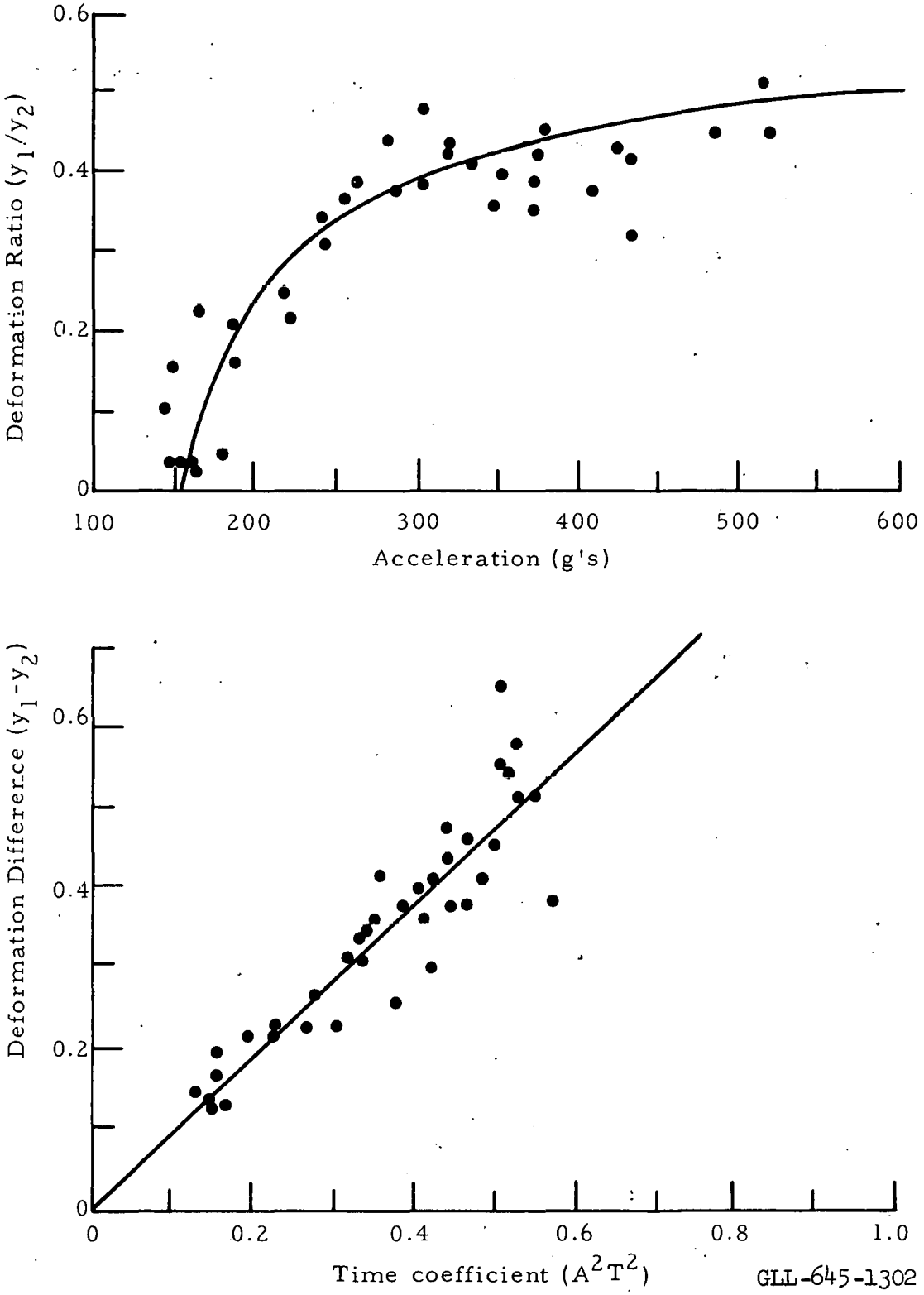

Fig. 12. Accelerometer data charts, mass ratio 2.0.

masses were taken out of their cases and accurately weighed, the Statham accelerometer was calibrated (see Appendix II for calibration method), and the effects of not quite perfectly square input wave shapes were investigated — all with no appreciable change in the existing results. It was then decided to make an accurate test on the honeycomb coupon material and determine whether or not there was any effect on its strength under varying strain rates. A preliminary calculation to ascertain what sort of crushing force would be required on the honeycomb to make it yield representative values in the two types of graphical plots results in two quite different values, neither of which was anywhere near previously measured figures. It was therefore decided that an accurate force-deflection record should be obtained for the material, since all such work up to that time had been done by reading a dial on a small mechanical testing machine and estimating average values.

A test was performed on an Instron testing machine, which has the capability of varying strain rates in a ten-to-one ratio by merely throwing a lever. This machine also utilizes a pen recorder to produce permanent test records. One of the masses was forced into the honeycomb in the test, so that force readings would correspond to the actual force that would oppose the plunger in the accelerometer.

This test had some interesting results, one of which did explain the deviation which had been observed. First of all, there was little or no effect due to varying strain rates, which agreed with other investigations on this subject (see Ref. 2). There was, as had been expected, an oscillation in the force-deflection curve, most likely arising from the buckling mechanism in the honeycomb. The factor that was unexpected, however, was the way the average force increased with deflection — a slope of approximately 5 pounds force increase per inch of deformation at an overall force level of about 55 pounds. This slope meant that the average force for any one deformation would increase as the deformation progressed, or, to be more specific, that each mass in the accelerometer would see a different average force in any one drop.

This slope could be handled mathematically with no great difficulty, but a complication arises in that the aforementioned oscillations in the crushing force have a maximum variation of approximately 15 pounds between maxima and minima, which could completely negate the effects of the slope in some instances and add to them in others. For this reason it was decided to use

the experimental data to calibrate the theoretical curves. This was accomplished by saying that the average force seen by the heavy mass was equal to the average force seen by the lighter mass plus a constant. Representative data points were then chosen from each of the experimental plots, and these, along with the above assumptions for deformation forces, were then inserted in the theoretical equations for the deformation ratio and the deformation difference. This gave two equations for two unknowns, namely the force seen by the light mass and the force seen by the heavy mass. In both cases, the force values which resulted fell within the range of deformation forces that had been recorded in the test on the honeycomb, so they were assumed to be realistic and were used to plot the theoretical curves in Figs. 11 and 12. The higher mass ratio showed the greatest difference in average forces (9 pounds versus 5 pounds), which is a logical result since the lighter mass ratio would always result in a greater difference in deformations for a given acceleration.

It is quite possible that a statistical survey of the honeycomb strength characteristics could be utilized to find the average crushing force for varying mass ratios, but time did not permit such an investigation for this project. Such methods could also be used to select more representative data points than were used here to calibrate the theoretical curves. The results which were obtained, however, are quite adequate for demonstrating the validity of the method.

Aside from the fact that a system such as this must be calibrated to find the crushing force characteristics, the experimental data shows that the system is quite capable of measuring acceleration levels and time pulse durations, as theoretically predicted.

The data points out some limitations, however, that were not at first apparent. First of all, there is a statistical scatter which runs as high as 25% due to variations in the strength of the honeycomb coupons. It is felt that this scatter could be reduced by using honeycomb manufactured to the more rigid military specifications and of a type having better dimensional control of the cell shapes. The cells in the material which was used (see Fig. 4) varied in shape from rectangular to hexagonal, which would cause the number of cell walls in the crushing area to vary. Another possibility would be to use a higher ratio of crushing area to cell size, thereby reducing variations in the percent of crushing area occupied by cell walls. Both of these ideas

fall into the category of "system optimization," an area where there is ample room for improvements.

Another more major limitation of this particular system lies in the shape of the deformation-ratio-versus-acceleration curve. It can be seen in Fig. 11 that rather good accuracy is achieved on the rise portion of this hyperbolic shape, but as the curve flattens out the accuracy is drastically reduced. This is due to the fact that a slight change in deformation ratio causes a large change in apparent acceleration in this area. The shape of this curve, therefore, has the effect of limiting the range of accelerations which can be indicated by the system. The time curve is not itself affected by this consideration, but a value must be known for the acceleration before one can be obtained for time.

A comparison of Figs. 11 and 12, however, indicates that there is some hope of at least minimizing this problem. A useful range of only 100-250 g's was achieved with a mass ratio of 1.3, but when the mass ratio was raised to 2.0 the range was extended to 150-450 g's. It appears that larger acceleration ranges can be obtained, therefore, by merely increasing the mass ratio. There are, undoubtedly, many applications where the acceleration ranges are known and small enough so that either of these mass ratios could be used, but a larger range would be desirable. Again, there is room for system optimization from this point of view.

A few drops were made upon lead cylinders at the end of the investigation. The idea here was to verify that this system would give values for an average acceleration and actual time length if the input pulse was not a square wave. The few drops that were so made — the input wave shape was triangular — indicated that the system did in fact react as predicted, although the aforementioned scatter was still in evidence. Further verification is required, however, before any positive conclusions can be drawn.

CONCLUSIONS

This system does fulfill the design objective which was set for it, namely that it measure the magnitude of acceleration and duration of time over which the acceleration is applied. There are certain limitations upon use of the system in its present form, but most of these could be improved upon or eliminated by changing some of the physical parameters of the system.

In addition to the primary objective mentioned above, secondary objectives of ruggedness and independence of external instrumentation were successfully met. Two other secondary objectives, compactness and reliability, were only partially satisfied. Further work in system optimization is needed to fully meet these other objectives.

Limited initial data indicates that the system will also react as predicted for non-square-wave acceleration inputs. Further verification is required before the system response to other types of inputs can be accurately predicted.

ACKNOWLEDGMENTS

Particular thanks are due Prof. G. Wayne Brown, of the University of California, for his invaluable guidance and assistance throughout the course of this design investigation.

The staff of the University of California Mechanics and Design Shop are to be credited for their skillful construction of the apparatus.

Thanks are due Mr. Dale Winter, of the Hexcel Corporation, for his gracious assistance in finding both information and material for the performance of this project.

Mr. Larry W. Lamoreux is to be commended for his excellent work in photographing the experimental facilities and equipment.

REFERENCES

1. "NOL Copper Ball Accelerometers," U. S. Naval Ordnance Laboratory Rept. 6638, May 1959.
2. "Energy Absorption Properties of Aluminum Honeycomb," Hexcel Products, Inc., Rept. TSB-110, January 1960.
3. Anders W. Lundberg, "A Peak Reading Accelerometer," Master of Engineering Design Project Rept., University of California, Berkeley, January 1961.
4. M. Hetenyi, Handbook of Experimental Stress Analysis (Wiley, New York, 1950).

APPENDIX I. ANALYSIS OF A NONLINEAR SPRING MASS SYSTEM

Nomenclature

Symbols

y	Deformation of honeycomb coupon
x	Linear motion of mass m or accelerometer case
m	Crusher mass in the accelerometer
F(t)	Crushing force on coupon (as function of time)
$\bar{F}$	Constant crushing force on coupon
A(t)	Input acceleration (as function of time)
A	Constant input acceleration (square wave)
V	Maximum velocity of deformation
Y	Total deformation
t	Time
σ	Honeycomb crushing strength (psi)

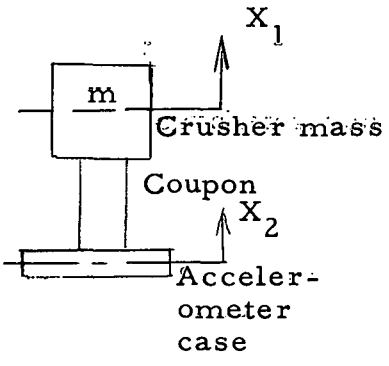

Fig. I-1

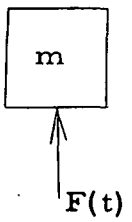

Fig. I-2

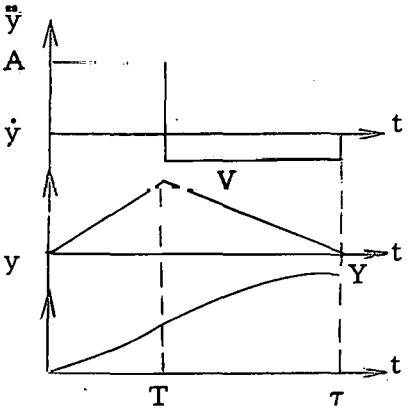

Fig. I-3

Idealized System

From Fig. I-1 we note that the deformation is

$$y = x_2 - x_1 \text{ (for } x_2 > x_1\text{)}.$$

Therefore

$$x_1 = x_2 - y$$

and

$$\ddot{x}_1 = \ddot{x}_2 - \ddot{y}. \tag{1}$$

Taking a force balance on the crusher mass (Fig. I-2), we obtain

$$\sum F = m\ddot{x}_1$$

or

$$F(t) = m\ddot{x}_1. \tag{2}$$

Combining (1) and (2) we obtain

$$m\ddot{x}_1 = m\ddot{x}_2 - m\ddot{y} = F(t), \tag{3}$$

which can be rewritten, noting that $\ddot{x}_2 = A(t)$ and that $F(t)$ = constant (for honeycomb coupon):

$$\ddot{y} = A(t) - F/m. \tag{4}$$

This equation, which is the equation of motion for the system, can now be solved by integrating twice, if the nature of $A(t)$ is known.

Let us assume that $A(t)$ is a square wave acceleration pulse, and, letting $A(t) = A$, plot the corresponding acceleration, velocity, and length of deformation curves (Fig. I-3). We are now interested in finding two things, time T and final deformation Y.

Making the first integration of Eq. (4), we obtain

$$\dot{y} = \int \ddot{y}\, dt = \int A\, dt - \frac{Ft}{m} \tag{5}$$

for which we have the boundary conditions:

$$\begin{aligned} &1)\ \dot{y} = V \text{ at } t = T \text{ (for } 0 \leq t \leq T), \\ &2)\ \dot{y} = 0 \text{ at } t = \tau \text{ (for } T \leq t \leq \tau). \end{aligned} \tag{6}$$

Applying boundary condition 2 we obtain

$$\dot{y} = AT - Ft/m$$

or

$$0 = AT - F\tau/m.$$

Therefore

$$\tau = m\Lambda T/F. \tag{7}$$

Now, applying boundary condition 1 we obtain

$$\dot{y} = (A - F/m)t$$

or

$$V = T\left(A - F/m\right). \tag{8}$$

Since we now know V and τ, and since the velocity curve is simply a triangle, we can now find the final deformation — which is the area under the velocity curve — by the relationship

$$\text{Area} = \frac{1}{2}\,(\text{base} \times \text{height})$$

or

$$\begin{aligned} y &= \frac{1}{2}\tau\left[T\left(A - \frac{F}{m}\right)\right] \\ &= \frac{1}{2}\left(\frac{mAT}{F}\right)\left[T\left(A - \frac{F}{m}\right)\right], \end{aligned}$$

and, finally,

$$y = \frac{1}{2}AT^2\left(\frac{Am}{F} - 1\right) \tag{9}$$

which is the equation for the total deformation of the coupon under a square-wave acceleration input.

We can now take Eq. (9) and combine it for two systems with two different masses, m_1 and m_2, to obtain an equation for the deformation ratio:

$$\frac{y_1}{y_2} = \frac{Am_1/F_1 - 1}{Am_2/F_2 - 1}, \tag{10}$$

which will plot graphically in the form of a hyperbola (Fig. I-4):

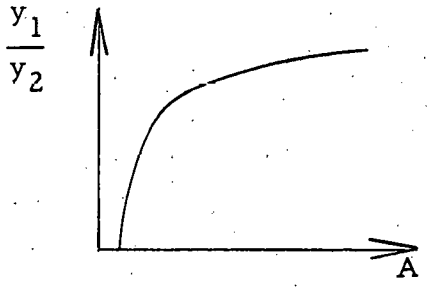

Fig. I-4

We can also obtain, by similar methods, an equation for the deformation difference:

$$(y_1 - y_2) = \frac{1}{2}A^2T^2\left[\frac{m_1}{F_1} - \frac{m_2}{F_2}\right]$$

which can be plotted graphically as a straight line (Fig. I-5):

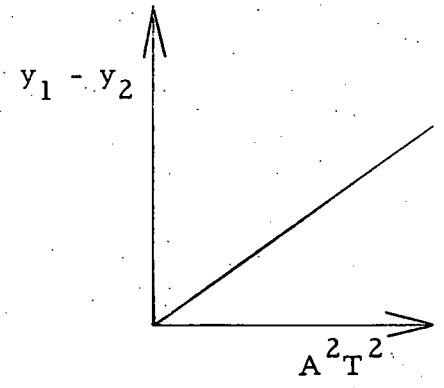

Fig. I-5

By using these two curves, then, it is possible to take the deformation from two systems and obtain values for the acceleration, A, and time, T. These are the two quantities which we have set out to measure.

APPENDIX II. CALIBRATION OF CONTROL ACCELEROMETER

The control citcuit, as shown in Fig. 9, consisted of a Statham accelerometer excited by an Ellis dc bridge power supply. The output from the power supply was fed into a Tektronix oscilloscope upon which was mounted a Polaroid camera for permanent recording of the traces. The Statham accelerometer is basically a fully external Wheatstone bridge, with four arms composed of unbounded resistance wire strain gages and with a temperature compensating parallel resistor on one of the arms. The output of this unit is proportional to accelerations along one of its axes.

The method which was used to calibrate this instrument was based on a drop being made from a known height, resulting in a known velocity at impact. A photograph was taken of the deceleration pulse trace, which was calibrated for time scale by the oscilloscope itself.

The trace was next blown up approximately 25 times, by projecting it on a vertical stand and going over its outline with a pencil. A polar planimeter was then utilized to obtain the blown-up area of the trace, which was divided by the length of time that the pulse had been applied. This gave an average trace height in centimeters, which was in turn divided into the calculated value of deceleration required to reduce the impact velocity to zero in the observed time. The resulting figure was the maximum sensitivity value for the entire control circuit. The value was 23.8 g's per centimeter of vertical deflection on the oscilloscope.